Size dependence of structural stability and magnetization of nickel clusters from real-space pseudopotentials

Masahiro Sakurai, Jaime Souto-Casares, and James R. Chelikowsky

Phys. Rev. B **94**, 024437 — Published 29 July 2016

DOI: 10.1103/PhysRevB.94.024437

Size dependence of stability and magnetization of nickel clusters from real-space pseudopotentials

Masahiro Sakurai[1], Jaime Souto-Casares[1], James R. Chelikowsky[1,2]
[1] *Center for Computational Materials, Institute for Computational Engineering and Sciences, University of Texas at Austin, Austin, Texas 78712, USA,*
[2] *Departments of Physics and Chemical Engineering, University of Texas at Austin, Austin, Texas 78712, USA.*
(Dated: July 12, 2016)

We examine the structural stability and magnetization for nickel clusters containing up to 500 atoms by performing first-principles calculations based on pseudopotential in real space computed within density-functional theory. After structural relaxation, Ni clusters in this size range favor either face-centered cubic (fcc) structure, which is a crystal structure in bulk, or icosahedral structure, which is expected for small clusters. The calculated total magnetic moments per atom of energetically stable clusters agree well with experiment, wherein the moments decrease non-monotonically toward the bulk value as cluster size increases. We analyze the spatial distribution of the local magnetic moment, which explains why the magnetic moments of Ni clusters are enhanced compared to their bulk value.

PACS numbers: 75.50.-y, 75.75.-c, 36.40.Cg, 63.22.Kn

I. INTRODUCTION

Magnetism in 3*d* transition metals is a central property, which has been intensively studied since the invention of quantum mechanics. In particular, ferromagnetism in 3*d* transition-metal nanoclusters, which can be described by the itinerant electron model,[1] has attracted interest not only from the viewpoint of fundamental physics, but also because of potential technological applications such as high-density magnetic data storage.[2] Also, transition-metal nanoclusters have been of great interest as catalysts,[3] for example, for carbon nanotube growth.[4–6]

Stern-Gerlach deflection experiments[7–9] first established that atomic clusters of bulk ferromagnets of iron, cobalt, and nickel exhibit superparamagnetic behavior[10,11], where the cluster can be regarded as a single-domain ferromagnetic particle. Experiment revealed that in such clusters the magnetic moments per atom exhibit a non-monotonic oscillatory decrease as a function of cluster size, converging to corresponding bulk values near cluster sizes of 500–700 atoms. Compared to the bulk, atoms on the surface of a cluster have low coordination, leading to weaker hybridization among 3*d* orbitals resulting in narrow 3*d* electronic band structures. This results in an increase of the difference in electron population between majority (spin-up) and minority (spin-down) electrons and qualitatively accounts for an enhancement of the magnetic moments observed for these clusters within this size range. As shown in our previous work on Fe and Co clusters,[12–14] the structural and magnetic properties of 3*d* transition-metal clusters depend strongly on their geometrical structures such as local coordination, surface morphology, and nucleation site.

Here we focus on Ni clusters. Since Ni prefers face-centered cubic (fcc) coordination, the size dependence of structural stability and magnetization of Ni clusters is expected to be different from those of clusters of Fe and Co, which favor body-centered cubic (bcc) coordination and hexagonal close-packed (hcp) coordination, respectively. For Ni, the existence of icosahedral cluster is suggested both theoretically[15] and experimentally,[16] although the details of the ground-state geometry of a cluster over a wide range of cluster sizes remains unknown. The convergent behavior of the magnetic moments of Ni clusters is believed to be slow, approximately attained for clusters with a minimum of 500–600 atoms.[7] Theoretical studies to date have been limited to specific Ni clusters with less than a few hundred atoms[17–19] owing to the lack of an accurate, efficient numerical method for calculating the electronic structures of large clusters.

Here, we employ a first-principles real-space pseudopotential method to predict the structural stability and magnetization of Ni clusters containing up to 500 atoms. Our work covers a broad range in size from small clusters, with atomic-like enhanced magnetic moments, to large clusters, with magnetization approaching the bulk limit. We discuss the influence of crystal structure manifolds on stability and the magnetic moment of Ni clusters. We carry out an analysis on the evolution of the local magnetic moment with respect to the radial distance and coordination number.

II. COMPUTATIONAL METHODS

We investigate the electronic structure of nickel clusters within the framework of the density-functional theory.[20,21] The exchange-correlation term is evaluated using the generalized gradient approximation (GGA) functional in the parameterized form of Perdew, Burke, and Ernzerhof,[22,23] which has been successfully applied to moderately correlated systems including transition-metal clusters.[12–14]

The Kohn-Sham equation is solved self-consistently using the PARSEC code.[24–27] The wave functions and the potentials are sampled on an uniform grid in *real space*. The kinetic term of the Hamiltonian is expanded by using a high-order finite-differencing.[24–26] We use norm-conserving pseudopotentials, constructed within the Troullier-Martins formalism[28] to describe the interactions between core and valence electrons. We choose a reference configuration of $[Ar]3d^8 4s^2 4p^0$ and core radii of $r_s = 2.18$, $r_p = 2.38$, and $r_d = 2.18$ a.u. (1 a.u. = 0.5292 Å), respectively, and include a partial core-correction as in our previous work.[14] Real space methods offer advantages over methods that employ an explicit basis, *e.g.*, they do not require the use of supercells for confined systems and like plane waves contain only one convergence parameter– the grid space size. We adopt a "cluster" boundary condition that requires the wave functions to vanish outside a spherical domain encompassing cluster of interest. The radius of the boundary sphere is typically 10 a.u. larger than that of the nickel cluster. We use periodic boundary conditions[27] only for computing bulk quantities. Our grid spacing was taken to be 0.29 a.u., which gives a total energy converged to within 0.01 eV/atom. Structural relaxations are performed using the Broyden-Fletcher-Goldfarb-Shanno method[29–31] with a residual force tolerance of 0.01 Ry/a.u.

Solving the Kohn-Sham equation involves constructing a self-consistent field (SCF) solution, which is obtained iteratively. Each SCF iteration requires a diagonalization of the Hamiltonian matrix, the most time-consuming part of computation. We avoid an explicit diagonalization by employing Chebyshev-filtered subspace iteration,[32,33] which at most requires one explicit diagonalization at the first SCF step and then improves eigenvectors at and after the second step. This filtering method, implemented in the current version of PARSEC, reduces computational time by at least one order of magnitude with respect to previous versions of the code.[34] Moreover, PARSEC enjoys the benefit of massive parallelization, making it feasible to compute the electronic structures of magnetic clusters containing hundreds of atoms.[14]

III. GEOMETRY

To investigate the role of crystal structure in determining stability and magnetic properties of Ni clusters, we consider three archetypical structures: icosahedron, face-centered cubic (fcc), and body-centered cubic (bcc). The icosahedral geometry is predicted to be stable up to 2,000 Ni atoms[15] and the photoionization experiment with time-of-flight mass spectrometry[16] suggests the existence of icosahedral clusters with hundreds of atoms. We construct an initial icosahedral Ni cluster so that the nearest-neighbor atomic distance of the cluster interior is equal to that of bulk fcc Ni. Since Ni favors an fcc crystal structure in the bulk, we explore two nucleation centers for fcc Ni clusters: atom-centered clusters and interstice-centered ones. The former has one Ni atom at the center of a cluster, and the latter is centered on the body center (an "interstitial" site) of the fcc unit cell. The lattice parameter of an fcc Ni cluster at the initial relaxation step is equal to the bulk value, 3.52 Å. Some of the fcc clusters possess 8 triangular faces and 6 square faces with cuboctahedral symmetry. While the fcc phase of Ni is thermodynamically stable at room temperature, the bcc phase has been produced in the form of thin films on a GaAs substrate.[35] In atomic clusters, the surface area is so large that bcc Ni cluster is expected to be stabilized under certain growth conditions. We study atom-centered geometry for bcc clusters with the initial lattice parameter taken from the experimental value, 2.82 Å. We examined a total of 61 Ni clusters, with 490 atoms being the largest one, consisting of 14 icosahedral, 16 atom-centered fcc, 13 interstice-centered fcc, and 18 bcc clusters.

IV. RESULTS

A. Stability

We carried out structural relaxations for clusters with up to 309 atoms. The total energies of unrelaxed and relaxed Ni clusters are plotted in Figs. 1(a) and (b), respectively, as a function of the cluster size. The dashed curve is a polynomial fit to the result of icosahedral clusters. The total energy of bulk fcc Ni, set as an energy reference in the plots, is evaluated using the same Ni pseudopotential and a k-point sampling with 16^3 grid.

As expected, the total energy of cluster generally decreases as cluster grows in size, approaching to the bulk value. However, the decrease of the total energy is not monotonic. The oscillatory behavior is associated with the cluster shape and surface geometry. For example, local minima in energy are found for the icosahedral family at sizes of 55, 147, and 298. These numbers correspond to perfect (55 and 147) and nearly-perfect (298) icosahedra, respectively. These icosahedral clusters are stable among the clusters with similar sizes, being consistent with the experimental observations.[16] The relatively high stability of perfect and nearly-perfect icosahedra was also found in our work on Co clusters.[14] Since the icosahedral cluster has an fcc coordination in each triangular face, icosahedral and fcc clusters are energetically competing with each other in the size range of our work. In contrast, bcc clusters tend to be higher in energy than icosahedral and fcc ones. This trend is remarkable for geometry-relaxed clusters, for energy gain due to structural relaxation is larger in icosahedral clusters than in bcc ones. By inspecting the total energies of relaxed clusters, we can extract energetically stable clusters from four structural families: icosahedron with 55, 135, 147, 237, and 297 atoms; atom-centered fcc with 43, 79, and 201 atoms;

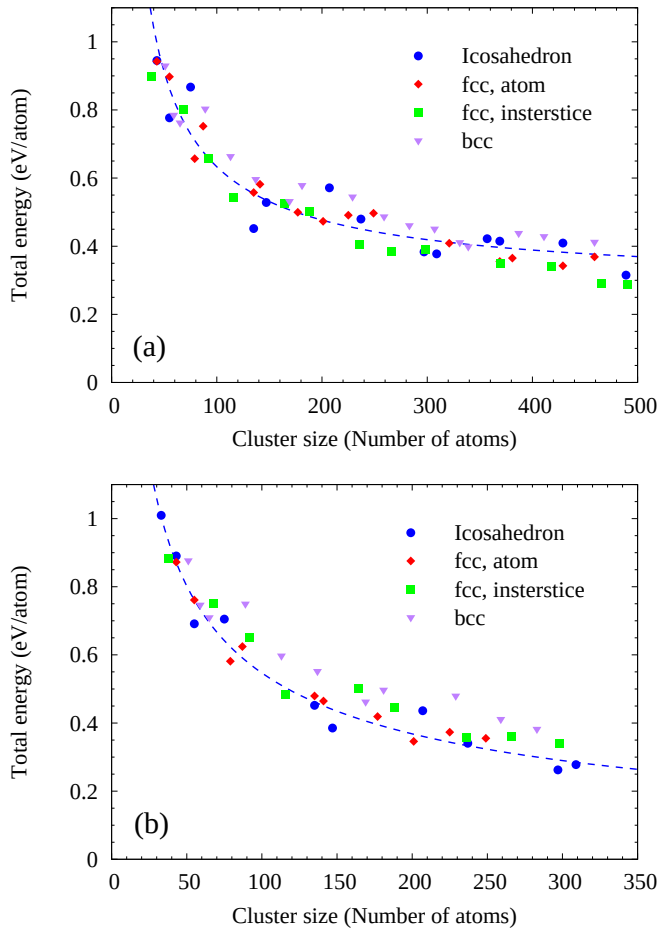

FIG. 1: Total energies of (a) unrelaxed and (b) relaxed Ni clusters as a function of cluster size. Energy is measured from that of bulk fcc Ni.

and interstice-centered fcc with 38 and 116 atoms. The results of unrelaxed clusters indicate the dominance of fcc structures for large clusters with more than 400 atoms.

B. Total Magnetic Moments

First, we examine the energetic order of paramagnetic and ferromagnetic systems for four representative Ni clusters: 55-atoms icosahedron, atom-centered fcc with 43 atoms, interstice-centered fcc with 38 atoms, and bcc with 51 atoms. We find that in all cases the ferromagnetic configuration is lower in energy than the paramagnetic one, indicating that the present pseudopotential method with the GGA-PBE functional is capable of describing the ferromagnetic behavior of Ni clusters.

Spin imbalance between majority and minority spins results in a magnetic moment, $\langle S_z \rangle$, which dominates the net magnetic moment in transition-metal clusters. In addition, spin-orbit coupling produces an orbital magnetic moment, $\langle L_z \rangle$, which makes an additive, posi-

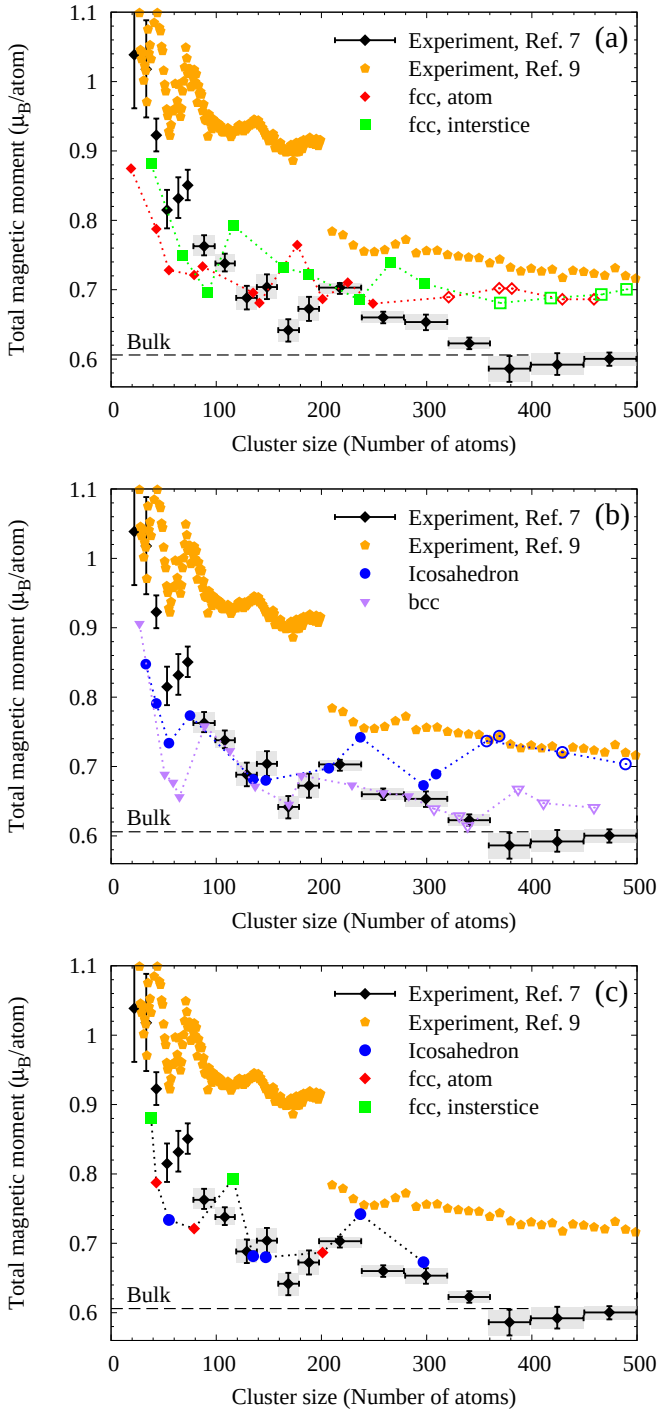

FIG. 2: Size dependence of the total magnetic moment per atom of various Ni clusters: (a) atom-centered and interstice-centered fcc clusters, (b) icosahedral and bcc clusters, and (c) energetically stable clusters (see text). The calculated moments, with filled (open) symbols for geometry-relaxed (unrelaxed) clusters, are compared to the experimental data[7,9]. The shaded region covers the range of the error bars. The dashed line indicates the total magnetic moment per atom of bulk fcc Ni (0.606 μ_B/atom).

tive contribution. The total magnetic moment, M, is given by a sum of the spin and orbital moments, $M = [g_s\langle S_z\rangle + \langle L_z\rangle]\mu_B$, with $g_s = 2$ being the electron gyromagnetic ratio and μ_B the Bohr magneton. In bulk fcc Ni, orbital effects result in an effective gyromagnetic ratio of $g_{\rm eff} = M/\langle S_z\rangle = 2.18\mu_B$. In this work, we consider the spin moment only and neglect the orbital moment for the sake of simplicity. We note that the present real-space pseudopotential calculation gives the spin moment of 0.58 μ_B for bulk fcc Ni, which is only slightly smaller than the experimental moment (0.606 μ_B).

Structural relaxation induces a slight alteration of the bond length of Ni atoms mainly near the surface of a cluster. This alteration leads to a weakening or strengthening hybridization of $3d$ orbitals, resulting in change of populations of the majority and minority spins. The change in the spin moment after structural relaxation ranges from a $\sim$2% decrease to an $\sim$2% increase compared to the value of the unrelaxed structure.

The size dependences of the total magnetic moment per atom for various Ni clusters are shown in Figs. 2(a)–(c), where the calculated moments are compared to the experimental data for clusters with up to 500 atoms. Filled (open) symbols represent the results of geometry-relaxed (unrelaxed) clusters. The discontinuity in the experimental data of Ref. 9 comes from two sets of measurements that were performed at different temperatures. The discrepancy of the measured moments between the two experiments may be attributed partly to the different temperatures as well as estimation of the cluster temperature, which is used to evaluate the effective magnetic moment through the Langevin function.

We find that the four structural families have two common features: (i) the total magnetic moment of clusters containing tens of atoms is significantly enhanced; (ii) As cluster grows in size, there is a gradual, non-monotonic decrease of the total magnetic moments, which is in overall agreement with the measured behaviors. A similar trend has been obtained experimentally and theoretically for clusters of Fe and Co.[7,12,14]

The total magnetic moments calculated for two families of fcc clusters are plotted in Fig. 2(a). For the clusters with more than 100 atoms, the calculated moments are in between the two experimental data. Two fcc families exhibit the local minimum (maximum) of the moment; its location depends on the nucleation center. For clusters containing more than 300 atoms, where the number of surface atoms per bulk atoms is noticeably reduced, the total magnetic moments of two fcc families essentially converge.

In Fig. 2(b), we compare the calculated total magnetic moments of the icosahedral family to experimental data. The calculated moments of the 55- and 147-atom icosahedral clusters agree well with the previous spin-polarized DFT calculation.[18] The local minimum and maximum moments are obtained at around sizes of 50 and 70, respectively, both of which agree qualitatively with experiment. The icosahedral clusters in the 80–300 atom range have moments in quantitative agreement with the measured moments of Ref. 7, while the large icosahedral clusters reproduce the measured ones of Ref. 9.

As shown in Fig. 2(b), bcc Ni clusters are predicted to have smaller total magnetic moment compared to fcc and icosahedral clusters. In bcc Ni clusters, the number of first nearest neighbors is reduced and the distance of first nearest-neighbor atoms is smaller than that of fcc ones. This leads to a stronger delocalization of the $3d$ orbitals, resulting in a reduction of the spin moment in the bcc Ni clusters. Although the bcc Ni cluster is predicted to be less stable according to our total-energy study, the bcc family unexpectedly reproduces the measured moments[7] for the size range of 90–340 including the pronounced dip in moments near a size of 170.

In Fig. 2(c), we summarize the total magnetic moments for the energetically stable clusters. Overall, the size dependence of the calculated moments agree with the experimental trend of Billas *et al.*[7] There is, however, a systematic underestimation for clusters containing less than $\sim$100 atoms. We speculate that this is due to omitting the orbital moment which arises from the spin-orbit coupling. In atomic cluster, the influence of the spin-orbit coupling on the orbital magnetization is expected to be different from that of bulk due to the presence of the surface. Considering that the present real-space pseudopotential calculation yields the spin moment that approximates to the experimental total moment for bulk fcc phase, and also for large clusters, our results suggest that the orbital moment could make a substantial contribution to the net magnetic moment in small Ni clusters.

C. Local Magnetic Moments

In order to analyze the local magnetic contributions to net magnetic moment of Ni clusters and their spatial distribution, we approximate a measure of the local magnetic moment as

$$m_j = \int_{\Omega_j} \left[\rho_\uparrow(\vec{r}) - \rho_\downarrow(\vec{r})\right] d^3\vec{r} \ .$$

Here, $\rho_{\uparrow(\downarrow)}$ denotes the electron density of the majority (minority) spin and Ω_j is a spherical domain centered on an atom labelled j. By definition, the local magnetic moment is a function of the distance from the cluster center, namely, $m_j = m(r_j)$. The radius of the sphere is chosen to be half of the minimum inter-atomic bond in the cluster. We confirm that the sum of the local magnetic moments ($\Sigma_j m_j$) approximates to the total magnetic moment (M) with a error less than $\sim$5%.

Fig. 3(a) shows the evolution of the local magnetic moment per atom of our four representative clusters, where the averaged local magnetic moment is plotted as a function of the radial distance. The local magnetic moment in the inner region of the icosahedral cluster is practically constant, with a bulk-like value, indicating that bulk-like environment is realized at deep inside of the cluster.

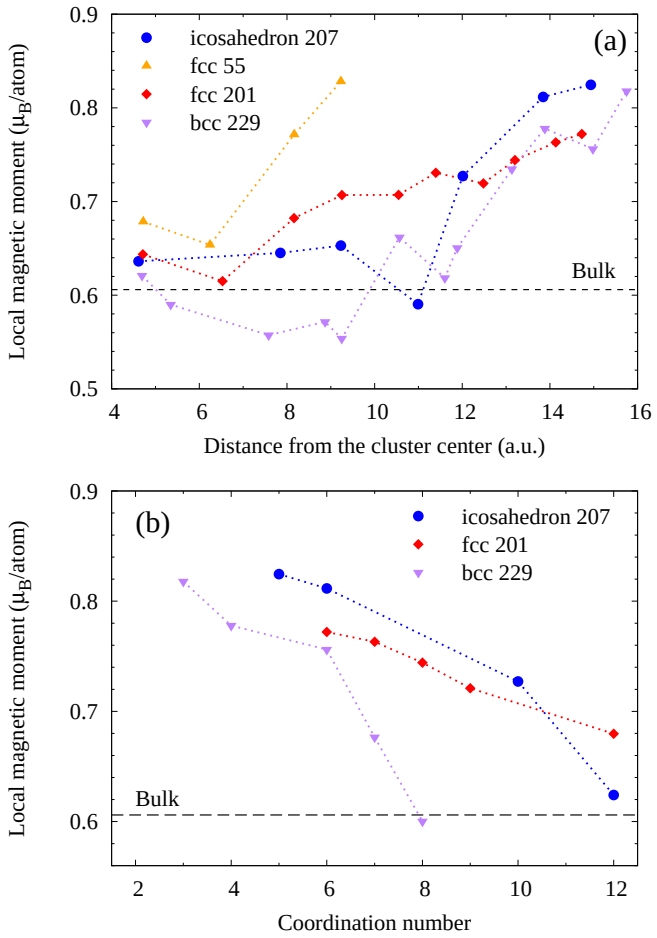

FIG. 3: Evolution of the local magnetic moment per atom as a function of (a) the distance from the cluster center and (b) the coordination number. The dashed line indicates the total magnetic moment per atom of bulk fcc Ni (0.606 μ_B/atom).

The icosahedral cluster shows strong growth of the local magnetic moment in the vicinity of surface, with a value comparable to the total magnetic moment per atom of the clusters containing tens of atoms. The increase of the local magnetic moments at the surface area of the bcc cluster is comparable to that of the icosahedral one, while the local magnetic moments of the interior region is suppressed. This explains why the calculated total magnetic moment of bcc clusters are smaller than those of icosahedral ones with similar sizes. The local magnetic moment of a smaller 55-atom fcc cluster is larger than that of the 201-atom cluster in the entire range of a radial distance from 4 a.u. to 10 a.u. This accounts for the enhancement of the net magnetic moment in small fcc clusters. This trend holds for small clusters with icosahedral and bcc structures.

In Fig. 3(b), we plot the local magnetic moment as a function of the coordination number. The plotted value is an average of several of the local magnetic moments (m_j) at various radial distances. Three representative clusters show a steady *increase* of the local magnetic moment as the coordination number *decreases*. The local magnetic moment of fcc cluster at a coordination number of 12 is slightly larger than that of bulk fcc Ni, indicating that the cluster interior is bulk-like, but the screening is likely incomplete owing to the presence of the surface. Although the growth rate of bcc cluster is virtually the same as that of icosahedral cluster, the local magnetic moment of bcc cluster is smaller at a specific coordination number. Moreover, the local magnetic moment of bcc cluster at a coordination number of eight converges to the value of bulk fcc Ni. This behavior reflects the smaller total magnetic moments that are predicted for bcc Ni clusters.

V. SUMMARY

We have studied the structural and magnetic properties of Ni clusters using the density-functional theory combined with real-space pseudopotentials. By examining the influence of cluster geometry on stability, we find that the icosahedral and fcc clusters are plausible structures for cluster sizes of up to 500 atoms. The overall size dependence of the total magnetic moments of the energetically stable clusters are consistent with the experiment. In particular, the stable clusters with hundreds of atoms are predicted to have the total magnetic moments that are within the range of the measured values. We have also provided an analysis on the evolution of the local magnetic moment with respect to a radial distance and coordination number, which explains the variation in the calculated magnetic moment.

Acknowledgments

This work is supported by the National Science Foundation, DMR 1435219. Computational resources have been provided by the Texas Advanced Computing Center (TACC) and the National Energy Research Scientific Computing Center (NERSC).

[1] D. C. Mattis, *The Theory of Magnetism* (Springer-Verlag, Berlin, 1988), 2nd ed.
[2] J. I. Martín, J. Nogués, K. Liu, J. L. Vicent, and I. K. Schuller, J. Magn. Magn .Mat. **256**, 449 (2003).
[3] C. R. Henry, Surf. Sci. Rep. **31**, 235 (1998).
[4] S. Iijima and T. Ichihashi, Nature (London) **363**, 603 (1993).
[5] D. S. Bethune, C. H. Kiang, M. S. de Vries, G. Gorman, R. Savoy, J. Vazquez, and R. Beyers, Nature (London) **363**, 605 (1993).

[6] A. Kasuya, Y. Sasaki, Y. Saito, K. Tohji, and Y. Nishina, Phys. Rev. Lett. **78**, 4434 (1997).
[7] I. M. L. Billas, A. Châtelain, and W. A. de Heer, Science **265**, 1682 (1994).
[8] I. M. L. Billas, A. Châtelain, and W. A. de Heer, J. Magn. Magn. Mater. **168**, 64 (1997).
[9] S. E. Apsel, J. W. Emmert, J. Deng, and L. A. Bloomfield Phys. Rev. Lett. **76**, 1441 (1996).
[10] C. P. Bean and J. D. Livingston, J. Appl. Phys. **30**, S120 (1959).
[11] S. N. Khanna and S. Linderoth Phys. Rev. Lett. **67**, 742 (1991).
[12] M. L. Tiago, Y. Zhou, M. M. G. Alemany, Y. Saad, and J. R. Chelikowsky, Phys. Rev. Lett. **97**, 147201 (2006).
[13] G. Rollmann, M. E. Gruner, A. Hucht, R. Meyer, P. Entel, M. L. Tiago, and J. R. Chelikowsky, Phys. Rev. Lett. **99**, 083402 (2007).
[14] J. Souto-Casares, M. Sakurai, and J. R. Chelikowsky, Phys. Rev. B **93**, 174418 (2016).
[15] C. L. Cleveland and U. Landman, J. Chem. Phys. **94**, 7376 (1991).
[16] M. Pellarin, B. Baguenard, J. L. Vialle, J. Lermé, M. Broyer, M. Miller, and A. Perez, Chem. Phys. Lett. **217**, 349 (1994).
[17] J. Guevara, F. Parisi, A. M. Llois, and M. Weissmann, Phys. Rev. B **55**, 13283 (1997).
[18] R. Singh and P. Kroll, Phys. Rev. B **78**, 245404 (2008).
[19] S. Sahoo, A. Hucht, M. E. Gruner, G. Rollmann, P. Entel, A. Postnikov, J. Ferrer, L. Fernandez-Seivane, M. Richter, D. Fritsch, and S. Sil, Phys. Rev. B **82**, 054418 (2010).
[20] P. Hohenberg and W. Kohn, Phys. Rev. **136**, B864 (1964).
[21] W. Kohn and L. Sham, Phys. Rev. **140**, A1133 (1965).
[22] J. P. Perdew, K. Burke, and M. Ernzerhof, Phys. Rev. Lett. **77**, 3865 (1996).
[23] J. P. Perdew, K. Burke, and M. Ernzerhof, Phys. Rev. Lett. **80**, 891 (1998).
[24] J. R. Chelikowsky, N. Troullier, and Y. Saad, Phys. Rev. Lett. **72**, 1240 (1994).
[25] J. R. Chelikowsky, N. Troullier, K. Wu, and Y. Saad, Phys. Rev. B **50**, 11355 (1994).
[26] L. Kronik, A. Makmal, M. L. Tiago, M. M. G. Alemany, M. Jain, X. Huang, Y. Saad, and J. R. Chelikowsky, Phys. Status Solidi **243**, 1063 (2006).
[27] A. Natan, A. Benjamini, D. Naveh, L. Kronik, M. L. Tiago, S. P. Beckman, and J. R. Chelikowsky, Phys. Rev. B **78**, 075109 (2008).
[28] N. Troullier and J. L. Martins, Phys. Rev. B **43**, 1993 (1991).
[29] R. H. Byrd, P. Lu, and J. Nocedal, SIAM J. Sci. Comput. **16**, 1190 (1995).
[30] C. Zhu, R. H. Byrd, and J. Nocedal, ACM Trans. Math. Software **23**, 550 (1997).
[31] J. L. Morales, and J. Nocedal, ACM Trans. Math. Software **38**, 1 (2011).
[32] Y. Zhou, Y. Saad, M. L. Tiago, and J. R. Chelikowsky, Phys. Rev. E **74**, 066704 (2006).
[33] Y. Zhou, Y. Saad, M. L. Tiago, and J. R. Chelikowsky, J. Comp. Phys. **219**, 172 (2006).
[34] K. H. Khoo, M. Kim, G. Schofield, and J. R. Chelikowsky, Phys. Rev. B, **82**, 064201 (2010).
[35] C. S. Tian, D. Qian, D. Wu, R. H. He, Y. Z. Wu, W. X. Tang, L. F. Yin, Y. S. Shi, G. S. Dong, X. F. Jin *et al.*, Phys. Rev. Lett. **94**, 137210 (2005).